

Linear-fitting-based recursive filtering for nonlinear systems under encoding-decoding mechanism

Bo JIANG^{1,2}, Hongli DONG^{1,2,4}, Zhiwei GAO³, Yuxuan SHEN^{1,2,4*} & Fan YANG^{1,2}¹Artificial Intelligence Energy Research Institute, Northeast Petroleum University, Daqing 163318, China;²Heilongjiang Provincial Key Laboratory of Networking and Intelligent Control, Daqing 163318, China;³School of Electrical & Information Engineering, Northeast Petroleum University, Daqing 163318, China;⁴Sanya Offshore Oil & Gas Research Institute, Northeast Petroleum University, Sanya 572024, China

Received 23 May 2023/Revised 29 August 2023/Accepted 5 October 2023/Published online 24 April 2024

Abstract This paper deals with a recursive filtering problem for a class of discrete time-varying nonlinear networked systems with the encoding-decoding mechanism. The linear fitting method is introduced to handle the nonlinearity. An encoding-decoding mechanism is constructed to describe the data transmission process in wireless communication networks (WCNs). To be specific, the measurement outputs are mapped by a quantizer to unique codewords for transmission in WCNs. Then, the codewords are decoded by the decoder to recover the measurement outputs which are sent to the filter. The processing/encoding delay and network delay have been considered. Firstly, on the premise that the upper bound of the filtering error covariance is minimum, the appropriate filtering gain is calculated. Then, the mean square exponential boundedness of the filtering error is analyzed. Finally, two simulation examples are presented to verify the effectiveness of the proposed algorithm.

Keywords encoding-decoding mechanism, uniform quantizer, linear fitting, networked systems, recursive filtering

1 Introduction

For the past few years, filtering problem has received numerous research enthusiasm in the field of signal processing and a great deal of excellent filtering algorithms have been proposed such as the Kalman filtering [1–3], the H_∞ filtering [4–6], the set membership filtering [7], and the particle filtering [8]. Among others, the Kalman filtering stands out for its high estimation accuracy and real-time computing ability [9,10]. Therefore, the Kalman filtering has been widely applied in missile guidance, radar tracking, aerospace, and many other fields. For example, the Kalman filtering has provided the theoretical basis for the feasibility of the famous Apollo space program implementation, especially for the vehicle-mounted navigation system [11]. A postprocessing algorithm using the Kalman filtering has been designed to forecast the weather more accurately [12].

As is known to all, the classic Kalman filtering is optimal for linear systems with Gaussian noises. Nevertheless, the systems in practical engineering are often nonlinear systems which lead to modifications of the classic Kalman filtering. Recently, the extended Kalman filtering (EKF) [13] and the unscented Kalman filtering (UKF) [14,15] are two common methods to resolve filtering problems for nonlinear systems. The EKF uses first-order Taylor expansion for linearization. Unfortunately, when the degree of nonlinearity is high, the neglect of the high-order terms may cause large linearization errors. The core idea of the UKF is using a group of weighted sigma points to calculate the predicted mean and variance after nonlinear transformation which is known as unscented transformation. The UKF is able to achieve the approximate second-order accuracy but does not obtain the Jacobian matrix of the nonlinear function. Note that, the Jacobian matrix is of great importance in some kinematic fields such as the instantaneous angular change of a manipulator. By combining the unscented transformation and the weighted least squares (WLS) method, the linear fitting algorithm (LFA) has been proposed in [16]. Compared with

* Corresponding author (email: shenyuxuan5973@163.com)

the EKF and the UKF, the LFA can obtain the Jacobian matrix of a nonlinear function and ensure the approximate second-order accuracy.

By means of the rise of digital communication, wireless communication networks (WCNs) have been widely applied due to the advantages of simple wiring, strong operability, and low power consumption [17, 18]. Despite the advantages of the WCNs, there are still certain limitations including limited network bandwidth and increasingly serious network security problems [19–24]. To deal with the limited network bandwidth, various communication protocols have been proposed, such as the event-triggering mechanism [25–31], the Try-Once-Discard protocol [32], and the random access protocol [33]. The core idea of these protocols is that the information transmissions are scheduled according to a given rule under which the valuable network sources are saved. Nevertheless, under these protocols, the transmitted data is still vulnerable to cyber attacks. For the purpose of enhancing bandwidth utilization and ensuring network security at the same time, research attention has been paid to the encoding-decoding mechanism (EDM) in recent years [34–36].

As the name implies, the EDM consists of two parts: encoder and decoder. In the encoding process, the measurement outputs are converted into completely different data, which can be regarded as a mapping process. These codewords are transmitted over WCNs to the decoder and then restored to approximate values of the original measurement outputs. Finally, the decoded outputs are sent to the filter for state estimation. It is pretty obvious that, under the EDM, only the codewords are transmitted over WCNs and hence the EDM provides a new way to solve the network security problem. As one of the most commonly used EDMs, the quantization-based EDM has recently received interest from researchers [37–41].

Under the EDM, due to the introduction of a quantizer in the encoding process, the decoded output will not be exactly the same as the original measurement output which brings additional challenges to the corresponding filtering/control problems [42–46]. In existing results, the research of quantization-based EDM in control has been fully considered while the filtering problems have received inadequate attention. The main reason is that it is difficult to find a correspondence between the actual measurement output and the decoded output. Meanwhile, due to the introduction of the quantizer, the quantization error will inevitably occur which may lead to the divergence of the filtering error. As such, the filtering problem under the quantization-based EDM still needs further research effort.

EDM usually contains two types of delays: processing/encoding delay and network delay [47]. Processing delay may result from detecting delay, computational delay, and other uncertainties of concerned events, and the network delay is mainly caused by the limited bandwidth in the communication network [48]. In other words, due to the processing/encoding delay, the codeword at the current time instant could correspond to the measurement output at a past time instant. Similarly, on account of the network delay, the decoded output at the current time instant could also correspond to the codeword at the past time instant. In the filtering problems, the overlook of such delays may degrade the filtering performance. Unfortunately, as far as we know, such a phenomenon has not been well considered which inspired the present study.

To summarize the above discussion, we focus on the problem of recursive filter design with EDM considering processing/encoding delay and network delay. The main challenges to be addressed are (1) how to construct a proper EDM to characterize the processing/encoding delay and network delay and (2) how to adequately take the error caused by the introduction of quantizer into account. To this end, the main contributions of this paper are (1) the LFA has been introduced to handle the considered nonlinear systems which perform better than the traditional methods; (2) a novel model has been proposed for the EDM with processing/encoding delay and network delay; and (3) the variance of the quantization error has been calculated which facilitates the subsequent filter design.

2 Problem formulation

Consider the following class of time-varying nonlinear systems:

$$x_{k+1} = h(x_k) + \mathcal{B}_k w_k, \quad (1)$$

$$z_k = \mathcal{C}_k x_k + v_k, \quad (2)$$

where $x_k \in \mathbb{R}^{n_x}$ is the system state and $z_k \in \mathbb{R}^{n_z}$ is the measurement output. w_k and v_k are the zero-mean Gaussian process noise and measurement noise with covariances $R_k > 0$ and $Q_k > 0$, respectively.

$h(\cdot)$ is a nonlinear function. \mathcal{B}_k and \mathcal{C}_k are known matrices. x_0 with the mean \bar{x}_0 and the covariance $\mathcal{P}_{0|0}$ is the initial value of the state x_k .

Remark 1. It is worth noting that when the nonlinear function is not differentiable or the nonlinear degree is large, the EKF will be inapplicable or generate a large linearization error. In addition, the UKF may not be able to obtain the Jacobian matrix of nonlinear functions. In this paper, we introduce the LFA based on unscented transformation to deal with the nonlinear function so as to achieve higher accuracy and obtain a Jacobian matrix at the same time.

2.1 Linear fitting algorithm

To handle the nonlinear function $h(\cdot)$, sigma points are first selected as follows:

$$\mathcal{X}_{k,1} = \hat{x}_{k|k}, \quad (3)$$

$$\mathcal{X}_{k,s} = \hat{x}_{k|k} + \left(\sqrt{(n_x + \kappa)\Theta_{k|k}} \right)_{s-1}, \quad \text{for } s = 2, \dots, n_x + 1, \quad (4)$$

$$\mathcal{X}_{k,s} = \hat{x}_{k|k} - \left(\sqrt{(n_x + \kappa)\Theta_{k|k}} \right)_{s-1-n_x}, \quad \text{for } s = n_x + 2, \dots, m, \quad (5)$$

where $\hat{x}_{k|k}$ is the state estimate defined later, $\Theta_{k|k}$ is the upper bound (UB) on the estimation error covariance, $(\sqrt{(n_x + \kappa)\Theta_{k|k}})_j$ is the j th column of $(\sqrt{(n_x + \kappa)\Theta_{k|k}})$, κ is a given scalar to determine the spread of sigma points, and $m = 2n_x + 1$.

Remark 2. Generally speaking, more sigma points are able to approximate the distribution of x_k more accurately at the cost of a larger computational burden. When the dimension of the system state is n_x , it is suggested to select $2n_x + 1$ sigma points. In addition, κ affects the high-order moment of the sigma points; thus an appropriate κ is helpful to reduce the overall approximate distribution error. It is suggested to select κ such that $n_x + \kappa = 3$ when the state is assumed Gaussian distribution [49].

After selection, the sigma points are mapped through a nonlinear function as [50]

$$\mathcal{X}_{k+1|k,i} = h(\mathcal{X}_{k,i}), \quad i = 1, \dots, m. \quad (6)$$

In order to minimize the error between the nonlinear function and its linearization, the WLS algorithm is introduced to calculate the linearized matrix H_k with the help of $\mathcal{X}_{k+1|k,i}$ as follows [16]:

$$H_k = \begin{bmatrix} H_{k,1} & H_{k,2} & \dots & H_{k,n_x} \end{bmatrix}^T \in \mathbb{R}^{n_x \times (n_x+1)}, \quad (7)$$

where

$$H_{k,i} \triangleq (\bar{\mathcal{X}}_k W \bar{\mathcal{X}}_k^T)^{-1} \bar{\mathcal{X}}_k W \bar{\mathcal{X}}_{k+1|k,i}^T, \quad i = 1, \dots, n_x,$$

$$\bar{\mathcal{X}}_k \triangleq \begin{bmatrix} \mathcal{X}_{k,1} & \mathcal{X}_{k,2} & \dots & \mathcal{X}_{k,m} \\ 1 & 1 & \dots & 1 \end{bmatrix} \in \mathbb{R}^{(n_x+1) \times m},$$

$$\mathcal{X}_{k+1|k} \triangleq \begin{bmatrix} \mathcal{X}_{k+1|k,1} & \mathcal{X}_{k+1|k,2} & \dots & \mathcal{X}_{k+1|k,m} \end{bmatrix} \in \mathbb{R}^{n_x \times m},$$

$$W \triangleq \text{diag}(\mathcal{W}_1, \mathcal{W}_2, \dots, \mathcal{W}_m),$$

$$\mathcal{W}_1 \triangleq \frac{\kappa}{n_x + \kappa}, \quad \mathcal{W}_s \triangleq \frac{1}{2(n_x + \kappa)}, \quad s = 2, \dots, m,$$

and $\bar{\mathcal{X}}_{k+1|k,i}$ is the i th row of $\mathcal{X}_{k+1|k}$. Considering the structure of $\bar{\mathcal{X}}_k$, we remove the last column of H_k to obtain the \mathcal{H}_k equal to the numerical Jacobian matrix of nonlinear function [16]:

$$H_k \rightarrow \mathcal{H}_k \in \mathbb{R}^{n_x \times n_x}.$$

Thus, for the state model (1), the approximate linearized state model is written as

$$x_{k+1} = \mathcal{H}_k x_k + \mathcal{B}_k w_k. \quad (8)$$

Remark 3. Up to now, the nonlinear function $h(\cdot)$ has been linearized by using the LFA and achieves a second-order approximation accuracy [51]. Unlike the UKF, which uses sigma points to directly calculate the posterior mean and variance, the LFA uses the WLS method to derive the Jacobian matrix of the nonlinear function to obtain the posterior mean and variance. It is worth noting that the numerical Jacobian is of great significance when a nonlinear function has an incomplete analytic expression.

2.2 Encoding-decoding mechanism

During the data transmission, network security and bandwidth limitation are two great concerns which need to be seriously taken into account. The EDM is an effective way to handle these two concerns. In recent studies on the EDM, it is often assumed that the encoding and decoding processes are completed at the same time instant. Unfortunately, both the processing/encoding delay and network delay are able to affect the filtering performance. In this case, the assumption that the encoding and decoding processes are completed at the same time instant is unrealistic and it is of great significance to consider the processing/encoding delay and network delay.

By taking into account the time spent in the encoding process and the network transmission process, the encoder is defined as follows:

$$s_k = q\left(\frac{1}{\eta_{k-d}}z_{k-d}\right), \quad (9)$$

where s_k is the codeword that is transmitted over the WCNs, $d > 0$ denotes the encoding delay, and $q(\cdot)$ is a uniform quantizer. $\eta_k > 0$ is a scaling function used to zoom in or out the measurement so that it falls within the range of the quantizer.

The form of the quantizer $q(\cdot)$ is shown below:

$$q(\chi) = \begin{cases} n, & \frac{2n-1}{2}\zeta \leq \chi < \frac{2n+1}{2}\zeta, n \in \{0, 1, \dots, l-1\}, \\ l, & \chi \geq \frac{2l-1}{2}\zeta, \\ -q(-\chi), & \chi < -\frac{1}{2}\zeta, \end{cases}$$

where ζ means the quantization interval and l is the saturation value of the quantizer.

Similarly, the decoder is defined as

$$\begin{cases} y_0 = 0, \\ y_k = \zeta\eta_{k-\tau-d}s_{k-\tau}, \end{cases} \quad (10)$$

where y_k is the decoding output received by the filter and τ denotes the network delay.

Remark 4. In EDM, due to the processing/encoding delay and network delay, the encoder and decoder will not work at the same time. d and τ represent the time required for the encoding process and the network transmission process, respectively. Note that, d and τ can be obtained from the prior knowledge and are assumed to be known in this paper.

In this paper, the recursive filter is designed in the following form:

$$\hat{x}_{k+1|k} = \mathcal{H}_k\hat{x}_{k|k}, \quad (11)$$

$$\hat{x}_{k+1|k+1} = \hat{x}_{k+1|k} + \mathcal{L}_{k+1}(y_{k+1} - \mathcal{C}_{k+1-u}\hat{x}_{k+1-u|k-u}), \quad (12)$$

where $\hat{x}_{k+1|k}$ and $\hat{x}_{k|k}$ are one-step prediction and the estimate of x_k at time instant k , respectively. $u \triangleq d + \tau$ represents the total time required for the encoding process and the network transmission process, and \mathcal{L}_{k+1} represents the filter gain to be designed subsequently.

$e_{k+1|k} \triangleq x_{k+1} - \hat{x}_{k+1|k}$ and $e_{k+1|k+1} \triangleq x_{k+1} - \hat{x}_{k+1|k+1}$ are defined as the prediction error and filtering error, respectively. Our main purpose is to design a recursive filter subject to the EDM considering processing/encoding delay and network delay and ensure that the filtering error covariance (FEC) has a minimal UB.

3 Main results

In this section, we are going to obtain the filter gain that minimizes the upper bound on the filtering error covariance. The following lemmas are given in advance to simplify the calculation.

Lemma 1 ([52]). For vectors $a \in \mathbb{R}^{n_a}$ and $b \in \mathbb{R}^{n_b}$, the following inequality holds:

$$ab^T + ba^T \leq \delta aa^T + \delta^{-1}bb^T, \quad (13)$$

where $\delta > 0$.

Lemma 2 ([53]). For given matrix $\mathfrak{X} = \mathfrak{X}^T > 0$ and two functions $\phi_k(\mathfrak{X}) = \phi_k^T(\mathfrak{X})$ and $\psi_k(\mathfrak{X}) = \psi_k^T(\mathfrak{X})$, if

$$\phi_k(\mathfrak{Y}) \geq \phi_k(\mathfrak{X}), \forall \mathfrak{X} \leq \mathfrak{Y} = \mathfrak{Y}^T,$$

and

$$\psi_k(\mathfrak{Y}) \geq \phi_k(\mathfrak{Y}),$$

then the solutions G_k and H_k of the following two difference equations:

$$G_{k+1} = \phi_k(G_k), H_{k+1} = \psi_k(H_k), G_0 = H_0 > 0,$$

satisfy $G_k \leq H_k$.

Lemma 3. For the uniform quantizer $q(\cdot)$, defining the quantization error as $D_k \triangleq \frac{1}{\eta_{k-d}} z_{k-d} - \zeta s_k$, one has

$$\text{Tr} \{ \mathbb{E} \{ D_{k-\tau} D_{k-\tau}^T \} \} = \sum_{i=1}^{n_z} \mathfrak{S}_{i,k-u},$$

where

$$\begin{aligned} \mathfrak{S}_{i,k-u} &\triangleq \begin{cases} \mathfrak{S}_{i,k-u|a}, & \text{for } y_{i,k} = n\zeta\eta_{k-u}, \\ \mathfrak{S}_{i,k-u|b}, & \text{for } y_{i,k} = l\zeta\eta_{k-u}, \\ \mathfrak{S}_{i,k-u|c}, & \text{for } y_{i,k} = -l\zeta\eta_{k-u}, \end{cases} \\ \mathfrak{S}_{i,k-u|a} &\triangleq \frac{\hbar_{i,k-u|a}}{\eta_{k-u}^2} - \frac{2n\zeta}{\eta_{k-u}} \aleph_{i,k-u|a} + (n\zeta)^2, \quad \mathfrak{S}_{i,k-u|b} \triangleq \frac{\hbar_{i,k-u|b}}{\eta_{k-u}^2} - \frac{2l\zeta}{\eta_{k-u}} \aleph_{i,k-u|b} + (l\zeta)^2, \\ \mathfrak{S}_{i,k-u|c} &\triangleq \frac{\hbar_{i,k-u|c}}{\eta_{k-u}^2} + \frac{2l\zeta}{\eta_{k-u}} \aleph_{i,k-u|c} + (l\zeta)^2, \quad \aleph_{i,k-u|a} \triangleq \mu_{i,k-u} - \sigma_{i,k-u}^2 \frac{o(\bar{\ell}_{k-u,n}) - o(\underline{\ell}_{k-u,n})}{O(\bar{\ell}_{k-u,n}) - O(\underline{\ell}_{k-u,n})}, \\ \aleph_{i,k-u|b} &\triangleq \mu_{i,k-u} + \sigma_{i,k-u}^2 \frac{o(\vartheta_{k-u})}{1 - O(\vartheta_{k-u})}, \quad \aleph_{i,k-u|c} \triangleq \mu_{i,k-u} - \sigma_{i,k-u}^2 \frac{o(-\vartheta_{k-u})}{O(-\vartheta_{k-u})}, \\ \hbar_{i,k-u|a} &\triangleq \sigma_{i,k-u}^2 \left[1 - \frac{\bar{\ell}_{k-u,n} o(\bar{\ell}_{k-u,n}) - \underline{\ell}_{k-u,n} o(\underline{\ell}_{k-u,n})}{O(\bar{\ell}_{k-u,n}) - O(\underline{\ell}_{k-u,n})} \right] + \mu_{i,k-u} \aleph_{i,k-u|a}, \\ \hbar_{i,k-u|b} &\triangleq \sigma_{i,k-u}^2 \left[1 + \frac{\vartheta_{k-u} o(\vartheta_{k-u})}{1 - O(\vartheta_{k-u})} \right] + \mu_{i,k-u} \aleph_{i,k-u|b}, \\ \hbar_{i,k-u|c} &\triangleq \sigma_{i,k-u}^2 \left[1 + \frac{\vartheta_{k-u} o(-\vartheta_{k-u})}{O(-\vartheta_{k-u})} \right] + \mu_{i,k-u} \aleph_{i,k-u|c}, \\ \underline{\ell}_{k-u,n} &\triangleq (2n-1)\zeta\eta_{k-u}/2, \quad \bar{\ell}_{k-u,n} \triangleq (2n+1)\zeta\eta_{k-u}/2, \quad \vartheta_{k-u} \triangleq (2l-1)\zeta\eta_{k-u}/2, \\ o(z_{i,k-u}) &\triangleq \frac{1}{\sqrt{2\pi}\sigma_{i,k-u}} e^{-\frac{(z_{i,k-u} - \mu_{i,k-u})^2}{2\sigma_{i,k-u}^2}}, \quad O(z_{i,k-u}) \triangleq \int_{-\infty}^{z_{i,k-u}} \frac{1}{\sqrt{2\pi}\sigma_{i,k-u}} e^{-\frac{(t - \mu_{i,k-u})^2}{2\sigma_{i,k-u}^2}} dt, \\ \mu_{i,k-u} &\triangleq (\mathcal{C}_{k-u} \hat{x}_{k-u|k-u-1})_i, \quad \sigma_{i,k-u}^2 = Q_{i,k-u}, \end{aligned}$$

$o(z_{i,k-u})$ and $O(z_{i,k-u})$ are the probability density function and the cumulative distribution function of $z_{i,k-u}$, respectively. $(\mathcal{C}_{k-u} \hat{x}_{k-u|k-u-1})_i$ is the i th component of $\mathcal{C}_{k-u} \hat{x}_{k-u|k-u-1}$ and $Q_{i,k-u}$ stands for the i th main diagonal element of Q_{k-u} .

Theorem 1. The recursive expressions of the one-step prediction error covariance $\mathcal{P}_{k+1|k} \triangleq \mathbb{E}\{e_{k+1|k} e_{k+1|k}^T\}$ and the FEC $\mathcal{P}_{k+1|k+1} \triangleq \mathbb{E}\{e_{k+1|k+1} e_{k+1|k+1}^T\}$ is shown below:

$$\mathcal{P}_{k+1|k} = \mathcal{H}_k \mathcal{P}_{k|k} \mathcal{H}_k^T + \mathcal{B}_k R_k \mathcal{B}_k^T \tag{14}$$

and

$$\mathcal{P}_{k+1|k+1}$$

$$\begin{aligned}
 &= \mathbb{E}\{(I - \mathcal{L}_{k+1}\mathcal{C}_{k+1})\mathcal{P}_{k+1|k}(I - \mathcal{L}_{k+1}\mathcal{C}_{k+1})^T + \mathcal{L}_{k+1}\mathcal{C}_{k+1}\mathcal{P}_{k+1|k}\mathcal{C}_{k+1}^T\mathcal{L}_{k+1}^T + \mathcal{L}_{k+1}\mathcal{Q}_{k+1-u}\mathcal{L}_{k+1}^T \\
 &\quad + \eta_{k+1-u}^2\mathcal{L}_{k+1}\mathbb{E}\{D_{k+1-\tau}D_{k+1-\tau}^T\}\mathcal{L}_{k+1}^T + \Upsilon_{1,k+1} + \mathcal{L}_{k+1}\mathcal{C}_{k+1-u}\mathcal{P}_{k+1-u|k-u}\mathcal{C}_{k+1-u}^T\mathcal{L}_{k+1}^T + \Upsilon_{1,k+1}^T \\
 &\quad - \Upsilon_{2,k+1} - \Upsilon_{2,k+1}^T + \Upsilon_{3,k+1} + \Upsilon_{3,k+1}^T - \Upsilon_{4,k+1} - \Upsilon_{4,k+1}^T + \Upsilon_{5,k+1} + \Upsilon_{5,k+1}^T \\
 &\quad - \Upsilon_{6,k+1} - \Upsilon_{6,k+1}^T - \Upsilon_{7,k+1} - \Upsilon_{7,k+1}^T\}, \tag{15}
 \end{aligned}$$

where

$$\begin{aligned}
 \Upsilon_{1,k+1} &\triangleq (I - \mathcal{L}_{k+1}\mathcal{C}_{k+1|k})e_{k+1|k}e_{k+1|k}^T\mathcal{C}_{k+1}^T\mathcal{L}_{k+1}^T, \\
 \Upsilon_{2,k+1} &\triangleq (I - \mathcal{L}_{k+1}\mathcal{C}_{k+1|k})e_{k+1|k}e_{k+1-u|k-u}^T\mathcal{C}_{k+1-u}^T\mathcal{L}_{k+1}^T, \\
 \Upsilon_{3,k+1} &\triangleq (I - \mathcal{L}_{k+1}\mathcal{C}_{k+1|k})e_{k+1|k}D_{k+1-\tau}^T\eta_{k+1-u}^T\mathcal{L}_{k+1}^T, \\
 \Upsilon_{4,k+1} &\triangleq \mathcal{L}_{k+1}\mathcal{C}_{k+1}e_{k+1|k}e_{k+1-u|k-u}^T\mathcal{C}_{k+1-u}^T\mathcal{L}_{k+1}^T, \\
 \Upsilon_{5,k+1} &\triangleq \mathcal{L}_{k+1}\mathcal{C}_{k+1}e_{k+1|k}D_{k+1-\tau}^T\eta_{k+1-u}^T\mathcal{L}_{k+1}^T, \\
 \Upsilon_{6,k+1} &\triangleq \mathcal{L}_{k+1}v_{k+1-u}D_{k+1-\tau}^T\eta_{k+1-u}^T\mathcal{L}_{k+1}^T, \\
 \Upsilon_{7,k+1} &\triangleq \mathcal{L}_{k+1}\mathcal{C}_{k+1-u}e_{k+1-u|k-u}D_{k+1-\tau}^T\eta_{k+1-u}^T\mathcal{L}_{k+1}^T.
 \end{aligned}$$

Proof. Taking (8) and (11) into consideration, one has

$$\begin{aligned}
 e_{k+1|k} &= x_{k+1} - \hat{x}_{k+1|k} \\
 &= \mathcal{H}_k x_k + \mathcal{B}_k w_k - \mathcal{H}_k \hat{x}_{k|k} \\
 &= \mathcal{H}_k e_{k|k} + \mathcal{B}_k w_k. \tag{16}
 \end{aligned}$$

From (10), (12), and the definition of quantization error, the filtering error $e_{k+1|k+1}$ is obtained as

$$\begin{aligned}
 e_{k+1|k+1} &= x_{k+1} - \hat{x}_{k+1|k+1} \\
 &= e_{k+1|k} - \mathcal{L}_{k+1}(z_{k+1-u} - \eta_{k+1-u}D_{k+1-\tau} - \mathcal{C}_{k+1-u}\hat{x}_{k+1-u|k-u}) \\
 &= (I - \mathcal{L}_{k+1}\mathcal{C}_{k+1})e_{k+1|k} + \mathcal{L}_{k+1}\mathcal{C}_{k+1}e_{k+1|k} - \mathcal{L}_{k+1}v_{k+1-u} \\
 &\quad - \mathcal{L}_{k+1}\mathcal{C}_{k+1-u}e_{k+1-u|k-u} + \mathcal{L}_{k+1}\eta_{k+1-u}D_{k+1-\tau}. \tag{17}
 \end{aligned}$$

Theorem 1 can be directly derived by (16) and (17).

Theorem 2. Given positive scalars $\alpha_1, \alpha_2, \alpha_3, \alpha_4, \alpha_5, \alpha_6,$ and $\alpha_7,$ on the premise that $\Theta_{0|0} \geq \mathcal{P}_{0|0} > 0,$ for the following two recursive matrix equations:

$$\Theta_{k+1|k} = \mathcal{H}_k \Theta_{k|k} \mathcal{H}_k^T + \mathcal{B}_k R_k \mathcal{B}_k^T \tag{18}$$

and

$$\begin{aligned}
 \Theta_{k+1|k+1} &= \delta_1(I - \mathcal{L}_{k+1}\mathcal{C}_{k+1})\Theta_{k+1|k}(I - \mathcal{L}_{k+1}\mathcal{C}_{k+1})^T + \delta_5\mathcal{L}_{k+1}\mathcal{C}_{k+1-u}\Theta_{k+1-u|k-u}\mathcal{C}_{k+1-u}^T\mathcal{L}_{k+1}^T \\
 &\quad + \delta_2\mathcal{L}_{k+1}\mathcal{C}_{k+1}\Theta_{k+1|k}\mathcal{C}_{k+1}^T\mathcal{L}_{k+1}^T + \delta_4\eta_{k+1-u}^2\sum_{i=1}^{n_z}\mathfrak{S}_{i,k+1-u}\mathcal{L}_{k+1}\mathcal{L}_{k+1}^T + \delta_3\mathcal{L}_{k+1}\mathcal{Q}_{k+1-u}\mathcal{L}_{k+1}^T, \tag{19}
 \end{aligned}$$

where

$$\begin{aligned}
 \delta_1 &\triangleq 1 + \alpha_1 + \alpha_2 + \alpha_3, \quad \delta_2 \triangleq 1 + \alpha_1^{-1} + \alpha_4 + \alpha_5, \quad \delta_3 \triangleq 1 + \alpha_6, \\
 \delta_4 &\triangleq 1 + \alpha_3^{-1} + \alpha_5^{-1} + \alpha_6^{-1} + \alpha_7^{-1}, \quad \delta_5 \triangleq 1 + \alpha_2^{-1} + \alpha_4^{-1} + \alpha_7,
 \end{aligned}$$

the solution $\Theta_{k+1|k+1}$ is an UB of $\mathcal{P}_{k+1|k+1}.$ Meanwhile, the filtering gain given below:

$$\mathcal{L}_{k+1} = \delta_1\Theta_{k+1|k}\mathcal{C}_{k+1}^T\mathcal{M}_{k+1}^{-1}, \tag{20}$$

where

$$\mathcal{M}_{k+1} \triangleq (\delta_1 + \delta_2)\mathcal{C}_{k+1}\Theta_{k+1|k}\mathcal{C}_{k+1}^T + \delta_3\mathcal{Q}_{k+1-u} + \delta_5\mathcal{C}_{k+1-u}\Theta_{k+1-u|k-u}\mathcal{C}_{k+1-u}^T + \delta_4\eta_{k+1-u}^2\sum_{i=1}^{n_z}\mathfrak{S}_{i,k+1-u}I,$$

ensures that $\Theta_{k+1|k+1}$ is minimal.

Algorithm 1 Recursive filtering algorithm with the EDM and LFA

- Step 1. Give the initial value $\hat{x}_{0|0}$, the initial value of the UB $\Theta_{0|0}$, and set $k = 0$.
 - Step 2. Calculate the linearized matrix \mathcal{H}_k with the help of (3)–(7).
 - Step 3. Obtain the one-step prediction $\hat{x}_{k+1|k}$ by (11).
 - Step 4. Compute the variance of quantization error D_{k+1} based on Lemma 3.
 - Step 5. Design the filter gain \mathcal{L}_{k+1} by (20). Obtain the minimum UB $\Theta_{k+1|k+1}$ on the FEC according to (19).
 - Step 6. Calculate the state estimate $\hat{x}_{k+1|k+1}$ by (12).
 - Step 7. Set $k = k + 1$ and go to Step 2.
-

Remark 5. As the EDM is introduced into the WCNs, the filtering performance will be affected by the parameters η_k , ζ , and \mathbf{u} . According to practical engineering experience, η_k can be dynamically selected to ensure that the encoded data fall within the quantizer range. Meanwhile, the quantization error decreases with the decrease of quantization interval ζ . In general, the more suitable η_k is selected, and the smaller the quantization interval is, the better the filtering performance gets. In addition, the bigger \mathbf{u} , that is, the larger the processing/encoding delay and network delay, the filter performance will be correspondingly worse.

Remark 6. Compared with other studies on the EDM, in this paper, the processing/encoding delay and network delay have been considered in the EDM, which is more practical. In addition, the previous studies usually ignore or limit quantization error, but in this paper, the variance of the quantization error has been calculated, which leads to the conservatism to some extent.

The specific recursive filtering algorithm is given in Algorithm 1.

4 Analysis of boundedness

In this section, we are committed to finding sufficient conditions for the filtering error to satisfy the mean-square exponential bounded (MSEB).

Lemma 4 ([54]). If stochastic process $V_k(\psi_k)$ and real numbers $\underline{\vartheta}$, $\overline{\vartheta}$, ρ , and $0 < \lambda < 1$ satisfy

$$\underline{\vartheta} \|\psi_k\|^2 \leq V_k(\psi_k) \leq \overline{\vartheta} \|\psi_k\|^2$$

and

$$\mathbb{E} \{V_k(\psi_k) | \psi_{k-1}\} \leq (1 - \lambda) V_{k-1}(\psi_{k-1}) + \rho,$$

then ψ_k is MSEB.

Theorem 3. Supposing there are positive numbers \underline{b} , \overline{b} , \underline{c} , \overline{c} , \underline{h} , \overline{h} , \underline{r} , \overline{r} , \underline{q} , \overline{q} , $\underline{\eta}$, $\overline{\eta}$, $\underline{\theta}$, $\overline{\theta}$, $\underline{\varpi}$, and $\overline{\varpi}$ that satisfy the following conditions:

$$\begin{aligned} \underline{h} &\leq \|\mathcal{H}_k\| \leq \overline{h} < 1, \quad \underline{b} \leq \|\mathcal{B}_k\| \leq \overline{b}, \quad \underline{c} \leq \|\mathcal{C}_k\| \leq \overline{c}, \\ \underline{r}I &\leq R_k \leq \overline{r}I, \quad \underline{q}I \leq Q_k \leq \overline{q}I, \quad \underline{\eta} \leq \eta_k \leq \overline{\eta}, \\ \underline{\theta}I &\leq \Theta_{k+1|k} \leq \overline{\theta}I, \quad \underline{\varpi}I \leq \Theta_{k+1|k+1} \leq \overline{\varpi}I, \end{aligned} \tag{21}$$

then the filtering error is MSEB.

Remark 7. So far, a recursive filter has been constructed with the EDM. By introducing the LFA with the WLS, the nonlinear function has been approximately linearized under the condition of minimum linearization error. In addition, an EDM model considering processing/encoding delay and network delay has been constructed to precisely reflect the working situation of the EDM. The variance of quantization error caused by the EDM has been calculated to improve the estimation accuracy. Then, a minimal UB on the FEC has been derived. Finally, we have analyzed the filtering error is MSEB. In Section 5, we present a simulation example and a numerical simulation.

5 Simulation examples

Example 1. In this simulation, we study a nonlinear pendulum system [55] for which the dynamical equations are given below:

$$\dot{\omega}(t) = \theta \overline{\omega}(t) + \alpha(t)((1 - \theta)\overline{\omega}(t) + \theta \omega(t)),$$

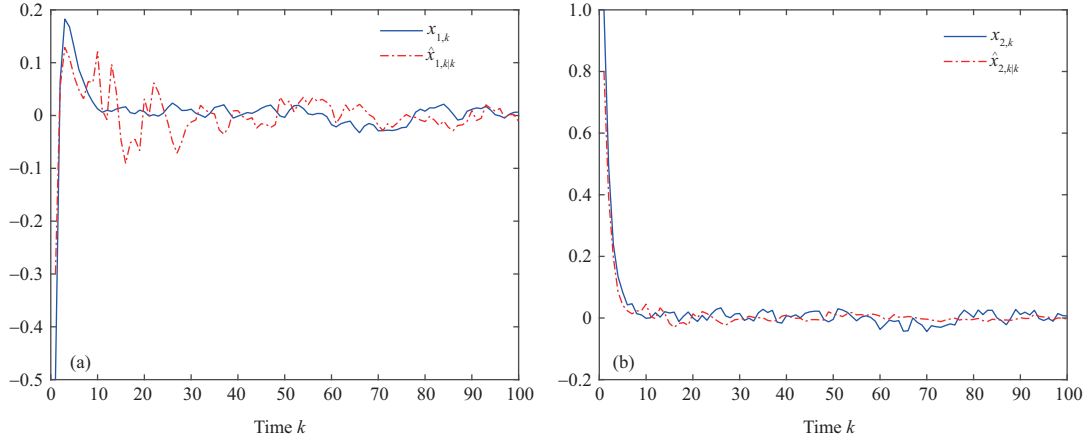


Figure 1 (Color online) (a) State $x_{1,k}$ and its estimate; (b) state $x_{2,k}$ and its estimate.

$$\dot{\bar{\omega}}(t) = -\frac{g \sin(\omega(t)) + (d/fm)\bar{\omega}(t) + (amf/4)\bar{\omega}(t)^2 \sin(2\omega(t))}{\frac{2f}{3} - \frac{a}{2}mf \cos(\omega(t))^2} - (amf\theta/4)w(t),$$

$$z(t) = \sin(\omega(t)) + \theta\bar{\omega}(t) + \theta v(t),$$

where ω is the angle of the pendulum in the vertical direction, $\bar{\omega}$ stands for the angular velocity. m and M are the mass of the pendulum and cart, respectively. g means the acceleration of gravity. f and d are the length of the pendulum and the associated damping coefficient, respectively. w and v are the interference acting on the cart and the noise produced in the measurement process, respectively. In this paper, specific parameters are selected as follows: $m = 2$ kg, $M = 8$ kg, $f = 0.5$ m, $d = 0.7$ N·m/s, $\theta = 0.6$, and sampling period $T = 0.02$ s. Letting $x_{1,t} = \omega(t)$ and $x_{2,t} = \bar{\omega}(t)$, the discrete-time pendulum system model is shown as follows:

$$x_{k+1} = h(x_k) + \mathcal{B}_k w_k,$$

$$z_k = \mathcal{C}_k x_k + \mathcal{D}_k v_k,$$

where

$$h(x_k) = \begin{bmatrix} 0.48x_{1,k} + 0.2x_{2,k} + 0.12 \sin(x_{2,k}) \\ 0.03x_{1,k} + 0.5x_{2,k} \end{bmatrix},$$

$$\mathcal{B}_k = \begin{bmatrix} 0.2 \\ 0.5 \end{bmatrix}, \mathcal{C}_k = \begin{bmatrix} -0.18 + 0.12 \sin(5k) & 0.48 \end{bmatrix}, \mathcal{D}_k = 0.28,$$

with $x_{i,k}$ ($i = 1, 2$) being the i th element of x_k .

In the simulation, $x_{0|0} = [-0.5 \ 1]^T$ and $\mathcal{P}_{0|0} = 2I \in \mathbb{R}^{2 \times 2}$. The covariances of w_k and v_k are chosen as $R_k = 0.01$ and $Q_k = 0.01$, respectively. $\eta_k = 0.08$, $\zeta = 0.16$, $d = 1$, $\tau = 1$, and $l = 12$. The mean square error (MSE) is defined as $\text{MSE} = \frac{1}{\mathcal{M}} \sum_{j=1}^{\mathcal{M}} \sum_{i=1}^2 (x_{i,k} - \hat{x}_{i,k|k})^2$ where $\mathcal{M} = 300$ is the number of simulation tests.

Figures 1(a) and (b) show the actual states $x_{i,k}$ ($i = 1, 2$) and estimated values $\hat{x}_{i,k|k}$ ($i = 1, 2$). Figures 2(a) and (b) visually show $\text{Tr}\{\Theta_k|k\}$ is larger than MSE and the filtering error is bounded, which implies the correctness of Theorems 2 and 3. Figure 3 depicts the actual measurement outputs are mapped to special codewords and transmitted over the WCNs, which means that it is difficult for attackers to steal valuable information and improves the security of the WCNs to a large extent.

Example 2. In this simulation, we are committed to highlighting the gap between the LFA and the Taylor expansion method (TEM), and also to showing the effect of the time required by the EDM on the filtering performance, with system parameters as follows:

$$h(x_k) = \begin{bmatrix} 0.73x_{2,k} - 0.6x_{1,k}x_{2,k} \\ 0.43 \sin(x_{1,k}x_{2,k}) + 0.6x_{2,k} \end{bmatrix}, \mathcal{B}_k = \begin{bmatrix} 0.5 \\ -0.7 + 0.1 \sin(0.2k) \end{bmatrix},$$

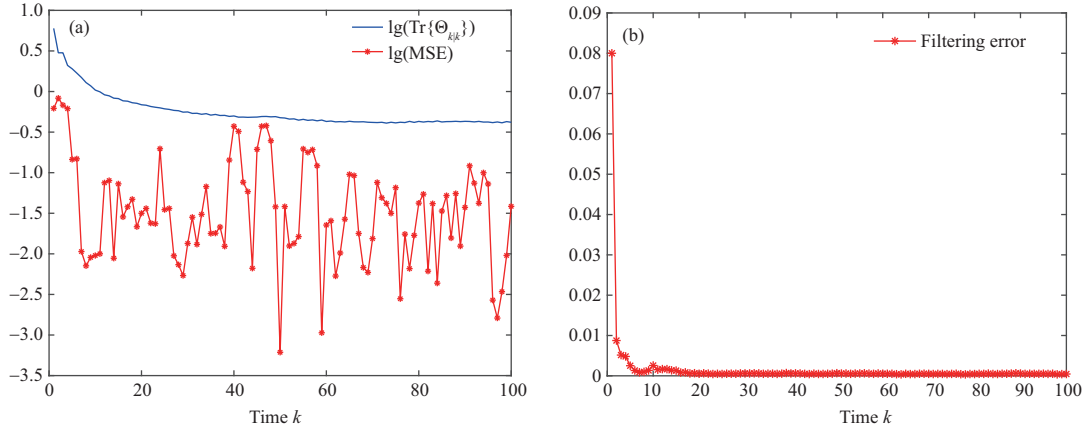


Figure 2 (Color online) (a) $\text{Tr}\{\Theta_{k|k}\}$ and the MSE; (b) filtering error.

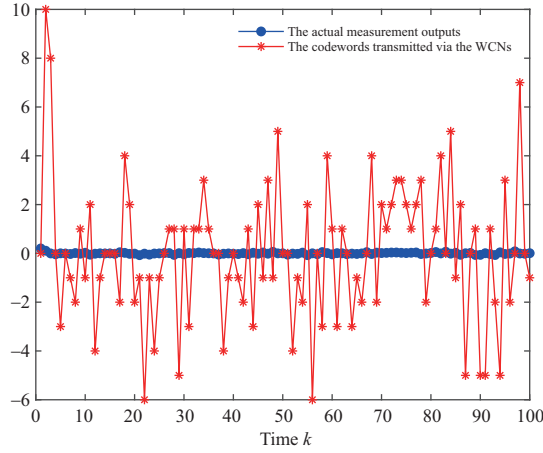


Figure 3 (Color online) Measurement outputs and compiled codewords.

$$\mathcal{C}_k = \begin{bmatrix} 0.6 + 0.01 \cos(2k) & 0 \\ 0 & 0.4 + 0.02 \sin(3k) \end{bmatrix}.$$

The rest of parameters are as follows: $x_{0|0} = [0.1 \ 0.2]^T$, $\mathcal{P}_{0|0} = 2I \in \mathbb{R}^{2 \times 2}$, $R_k = 0.01$, $Q_k = 0.01I \in \mathbb{R}^{2 \times 2}$, $\eta_k = 0.2$, $\zeta = 0.3$, $l = 10$, and $\mathcal{M} = 500$. In addition, for the purpose of intuitively reflecting the impact of the time required for EDM on the filtering performance, two cases are selected in this paper: case 1 is $d = 1$, $\tau = 1$ and case 2 is $d = 3$, $\tau = 3$.

Figures 4(a) and (b) represent the actual state curve and estimated value curve. Figure 4(c) plots the norm of filtering error. It is not difficult to find from Figure 4 that, compared with the TEM, the LFA has higher estimation accuracy and smaller filtering errors, which indicates that LFA has certain advantages in dealing with nonlinear problems. Similarly, Figure 4 shows that when the process delay and network delay increase, the filtering error will increase, resulting in a decrease in the estimation accuracy.

6 Conclusion

In this paper, the recursive filter has been designed which mainly includes nonlinear problem and the EDM considering encoding and decoding delays. The Jacobian matrix of the nonlinear function has been calculated using the LFA. In order to better describe the reality, an EDM with the process delay and network delay has been constructed to encrypt and compress measurement output to strengthen the security of WCNs. A suitable filter gain has been obtained to make that the UB of FEC is minimized.

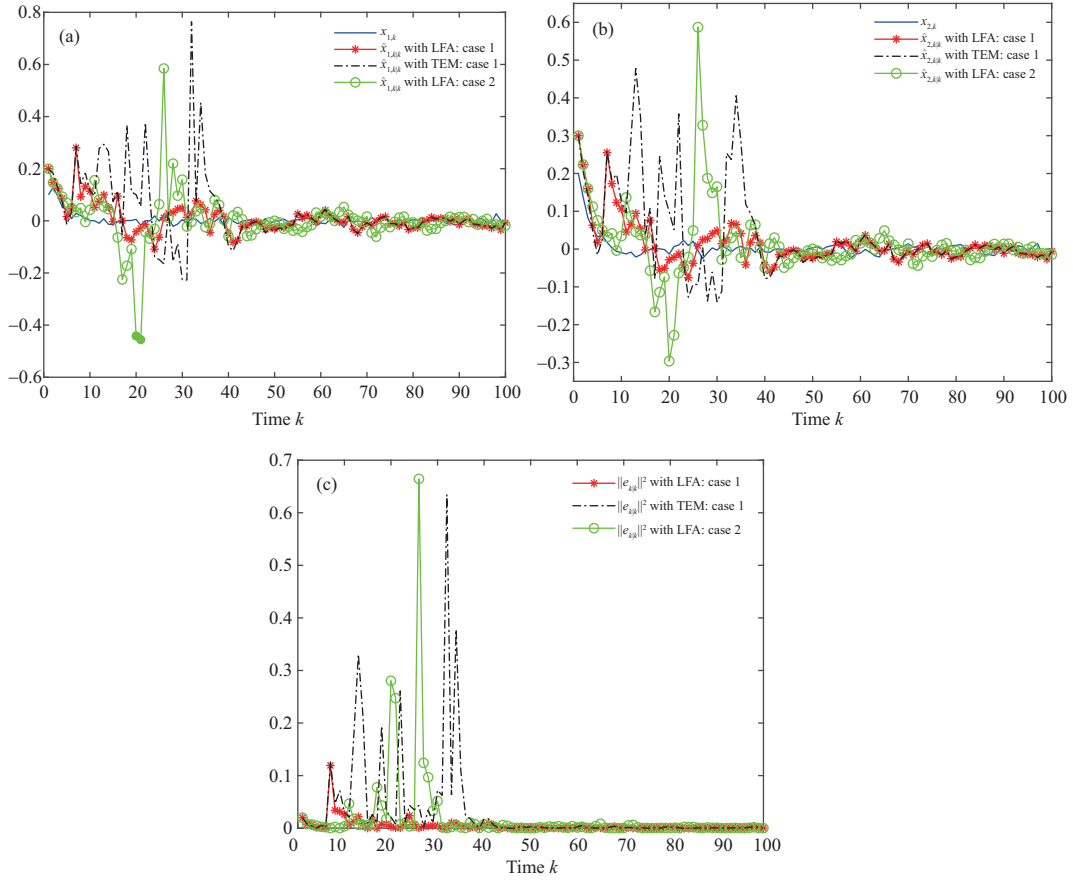


Figure 4 (Color online) (a) State $x_{1,k}$ and its estimate; (b) state $x_{2,k}$ and its estimate; (c) filtering error.

Moreover, sufficient conditions have been given to satisfy that the filtering error is MSEB. Finally, two simulation examples have been given to demonstrate the effectiveness of the designed algorithm.

Acknowledgements This work was supported in part by National Natural Science Foundation of China (Grant Nos. U21A2019, 61873058, 62103095), Hainan Province Science and Technology Special Fund (Grant No. ZDYF2022SHFZ105), Natural Science Foundation of Heilongjiang Province of China (Grant No. LH2021F005), and Alexander von Humboldt Foundation of Germany.

References

- 1 Gan D, Xie S Y, Liu Z X. Stability of the distributed Kalman filter using general random coefficients. *Sci China Inf Sci*, 2021, 64: 172204
- 2 Kalman R E. A new approach to linear filtering and prediction problems. *J Basic Eng*, 1960, 82: 35–45
- 3 Li X G, Feng S, Hou N, et al. Surface microseismic data denoising based on sparse autoencoder and Kalman filter. *Syst Sci Control Eng*, 2022, 10: 616–628
- 4 Chen Y, Zhu M Z, Lu R Q, et al. Distributed H_∞ filtering of nonlinear systems with random topology by an event-triggered protocol. *Sci China Inf Sci*, 2021, 64: 202204
- 5 Suo J H, Li N, Li Q. Event-triggered H_∞ state estimation for discrete-time delayed switched stochastic neural networks with persistent dwell-time switching regularities and sensor saturations. *Neurocomputing*, 2021, 455: 297–307
- 6 Wang N, Qian W, Xu X Z. H_∞ performance for load frequency control systems with random delays. *Syst Sci Control Eng*, 2021, 9: 243–259
- 7 Gollamudi S, Nagaraj S, Kapoor S, et al. Set-membership filtering and a set-membership normalized LMS algorithm with an adaptive step size. *IEEE Signal Process Lett*, 1998, 5: 111–114
- 8 Hlinka O, Slučiak O, Hlawatsch F, et al. Likelihood consensus and its application to distributed particle filtering. *IEEE Trans Signal Process*, 2012, 60: 4334–4349
- 9 Shen H, Huang Z G, Cao J D, et al. Exponential H_∞ filtering for continuous-time switched neural networks under persistent dwell-time switching regularity. *IEEE Trans Cybern*, 2019, 50: 2440–2449
- 10 Shrivastava P, Soon T K, Idris M Y I B, et al. Overview of model-based online state-of-charge estimation using Kalman filter family for lithium-ion batteries. *Renew Sustain Energy Rev*, 2019, 113: 109233
- 11 Schmidt S F. The Kalman filter — Its recognition and development for aerospace applications. *J Guidance Control*, 1981, 4: 4–7
- 12 Monache L D, Nipen T, Liu Y, et al. Kalman filter and analog schemes to postprocess numerical weather predictions. *Mon Weather Rev*, 2011, 139: 3554–3570
- 13 Hoshiya M, Saito E. Structural identification by extended Kalman filter. *J Eng Mech*, 1984, 110: 1757–1770
- 14 Hu G G, Gao B B, Zhong Y M, et al. Unscented Kalman filter with process noise covariance estimation for vehicular INS/GPS integration system. *Inf Fusion*, 2020, 64: 194–204

- 15 Julier S, Uhlmann J, Durrant-Whyte H F. A new method for the nonlinear transformation of means and covariances in filters and estimators. *IEEE Trans Automat Contr*, 2000, 45: 477–482
- 16 Xiong Y B, Zhong X H. Linear fitting Kalman filter. *IET Signal Process*, 2016, 10: 404–412
- 17 Ho Q D, Gao Y, Le-Ngoc T. Challenges and research opportunities in wireless communication networks for smart grid. *IEEE Wireless Commun*, 2013, 20: 89–95
- 18 You X H, Wang C-X, Huang J, et al. Towards 6G wireless communication networks: vision, enabling technologies, and new paradigm shifts. *Sci China Inf Sci*, 2021, 64: 110301
- 19 Liu S, Song Y, Wei G L, et al. RMPC-based security problem for polytopic uncertain system subject to deception attacks and persistent disturbances. *IET Control Theory Appl*, 2017, 11: 1611–1618
- 20 Tao H M, Tan H L, Chen Q W, et al. H_∞ state estimation for memristive neural networks with randomly occurring DoS attacks. *Syst Sci Control Eng*, 2022, 10: 154–165
- 21 Wang X L, Sun Y, Ding D R. Adaptive dynamic programming for networked control systems under communication constraints: a survey of trends and techniques. *Int J Network Dyn Intell*, 2022, 1: 85–98
- 22 Yao F, Ding Y L, Hong S G, et al. A survey on evolved LoRa-based communication technologies for emerging internet of things applications. *Int J Network Dyn Intell*, 2022, 1: 4–19
- 23 Yu L Y, Liu Y R, Cui Y, et al. Intermittent dynamic event-triggered state estimation for delayed complex networks based on partial nodes. *Neurocomputing*, 2021, 459: 59–69
- 24 Zou L, Wang Z D, Hu J, et al. Partial-node-based state estimation for delayed complex networks under intermittent measurement outliers: a multiple-order-holder approach. *IEEE Trans Neural Netw Learn Syst*, 2023, 34: 7181–7195
- 25 Alsaadi F E, Liu Y R, Alharbi N S. Design of robust H_∞ state estimator for delayed polytopic uncertain genetic regulatory networks: dealing with finite-time boundedness. *Neurocomputing*, 2022, 497: 170–181
- 26 Liu L, Zhao X D, Wang B H, et al. Event-triggered state estimation for cyber-physical systems with partially observed injection attacks. *Sci China Inf Sci*, 2023, 66: 169202
- 27 Qu F R, Zhao X, Wang X M, et al. Probabilistic-constrained distributed fusion filtering for a class of time-varying systems over sensor networks: a torus-event-triggering mechanism. *Int J Syst Sci*, 2022, 53: 1288–1297
- 28 Sun Y, Tian X, Wei G L. Finite-time distributed resilient state estimation subject to hybrid cyber-attacks: a new dynamic event-triggered case. *Int J Syst Sci*, 2022, 53: 2832–2844
- 29 Xiao H C, Ding D R, Dong H L, et al. Adaptive event-triggered state estimation for large-scale systems subject to deception attacks. *Sci China Inf Sci*, 2022, 65: 122207
- 30 Amini A, Asif A, Mohammadi A. Formation-containment control using dynamic event-triggering mechanism for multi-agent systems. *IEEE CAA J Autom Sin*, 2020, 7: 1235–1248
- 31 Liu J X, Wu L G, Wu C W, et al. Event-triggering dissipative control of switched stochastic systems via sliding mode. *Automatica*, 2019, 103: 261–273
- 32 Zhang Z N, Niu Y G, Lam H K. Sliding-mode control of T-S fuzzy systems under weighted try-once-discard protocol. *IEEE Trans Cybern*, 2019, 50: 4972–4982
- 33 Yu H Y, Hu J, Song B Y, et al. Resilient energy-to-peak filtering for linear parameter-varying systems under random access protocol. *Int J Syst Sci*, 2022, 53: 2421–2436
- 34 Shen B, Ding D R, Liu Q Y. Special issue on performance analysis and synthesis of networked systems under coding-decoding communication mechanisms. *Int J Syst Sci*, 2022, 53: 2709–2710
- 35 Wang L C, Wang Z D, Han Q L, et al. Synchronization control for a class of discrete-time dynamical networks with packet dropouts: a coding-decoding-based approach. *IEEE Trans Cybern*, 2017, 48: 2437–2448
- 36 Wang L C, Wang Z D, Wei G L, et al. Observer-based consensus control for discrete-time multiagent systems with coding-decoding communication protocol. *IEEE Trans Cybern*, 2018, 49: 4335–4345
- 37 Farhadi A, Ahmed N U. Tracking nonlinear noisy dynamic systems over noisy communication channels. *IEEE Trans Commun*, 2011, 59: 955–961
- 38 Liberzon D. On stabilization of linear systems with limited information. *IEEE Trans Automat Contr*, 2003, 48: 304–307
- 39 Liu Z T, Lin W Y, Yu X H, et al. Approximation-free robust synchronization control for dual-linear-motors-driven systems with uncertainties and disturbances. *IEEE Trans Ind Electron*, 2022, 69: 10500–10509
- 40 Savkin A V, Cheng T M. Detectability and output feedback stabilizability of nonlinear networked control systems. *IEEE Trans Automat Contr*, 2007, 52: 730–735
- 41 Wong W S, Brockett R W. Systems with finite communication bandwidth constraints. II. Stabilization with limited information feedback. *IEEE Trans Automat Contr*, 1999, 44: 1049–1053
- 42 Jin Z P, Gupta V, Murray R M. State estimation over packet dropping networks using multiple description coding. *Automatica*, 2006, 42: 1441–1452
- 43 Li T, Xie L H. Distributed consensus over digital networks with limited bandwidth and time-varying topologies. *Automatica*, 2011, 47: 2006–2015
- 44 Wen P Y, Li X R, Hou N, et al. Distributed recursive fault estimation with binary encoding schemes over sensor networks. *Syst Sci Control Eng*, 2022, 10: 417–427
- 45 Yu M, Yan C, Xie D M. Event-triggered control for couple-group multi-agent systems with logarithmic quantizers and communication delays. *Asian J Control*, 2017, 19: 681–691
- 46 Zou L, Wang Z D, Shen B, et al. Encrypted finite-horizon energy-to-peak state estimation for time-varying systems under eavesdropping attacks: tackling secrecy capacity. *IEEE CAA J Autom Sin*, 2023, 10: 985–996
- 47 Ling Q. Bit rate conditions to stabilize a continuous-time scalar linear system based on event triggering. *IEEE Trans Automat Contr*, 2017, 62: 4093–4100
- 48 Ling Q. Stabilizing bit rate conditions for a scalar continuous time linear system with bounded processing delay and bounded process noise. In: *Proceedings of the IEEE 55th Conference on Decision and Control, Las Vegas, 2016*. 4849–4854
- 49 Julier S, Uhlmann J. New extension of the Kalman filter to nonlinear systems. In: *Proceedings of SPIE*, 1997. 3068: 182–193
- 50 Zhang J H, Gao S S, Li G, et al. Distributed recursive filtering for multi-sensor networked systems with multi-step sensor delays, missing measurements and correlated noise. *Signal Processing*, 2021, 181: 107868
- 51 Xia J, Gao S S, Zhong Y M, et al. A novel fitting H-infinity Kalman filter for nonlinear uncertain discrete-time systems based on fitting transformation. *IEEE Access*, 2019, 8: 10554–10568
- 52 Hu J, Wang Z D, Liu G P, et al. Variance-constrained recursive state estimation for time-varying complex networks with quantized measurements and uncertain inner coupling. *IEEE Trans Neural Netw Learn Syst*, 2020, 31: 1955–1967
- 53 Theodor Y, Shaked U. Robust discrete-time minimum-variance filtering. *IEEE Trans Signal Process*, 1996, 44: 181–189

- 54 Reif K, Gunther S, Yaz E, et al. Stochastic stability of the discrete-time extended Kalman filter. *IEEE Trans Automat Contr*, 1999, 44: 714–728
- 55 Dong H L, Wang Z D, Ding S X, et al. On H_∞ estimation of randomly occurring faults for a class of nonlinear time-varying systems with fading channels. *IEEE Trans Automat Contr*, 2015, 61: 479–484

Appendix A Proof of Lemma 3

By using the properties of truncated Gaussian, for $z_{i,k-u} \in [\underline{\ell}_{k-u,n}, \bar{\ell}_{k-u,n})$, one has

$$\begin{aligned} & \mathbb{E} \left\{ z_{i,k-u} \mid z_{i,k-u} \in [\underline{\ell}_{k-u,n}, \bar{\ell}_{k-u,n}), x_{k-u} \right\} \\ &= \int_{\underline{\ell}_{k-u,n}}^{\bar{\ell}_{k-u,n}} z_{i,k-u} \frac{o(z_{i,k-u})}{O(\bar{\ell}_{k-u,n}) - O(\underline{\ell}_{k-u,n})} dz_{i,k-u} \\ &= \frac{\mu_{i,k-u}}{O(\bar{\ell}_{k-u,n}) - O(\underline{\ell}_{k-u,n})} \int_{\underline{\ell}_{k-u,n}}^{\bar{\ell}_{k-u,n}} o(z_{i,k-u}) dz_{i,k-u} - \frac{\sigma_{i,k-u}^2 \int_{\underline{\ell}_{k-u,n}}^{\bar{\ell}_{k-u,n}} \frac{-(z_{i,k-u} - \mu_{i,k-u})}{\sigma_{i,k-u}^2} o(z_{i,k-u}) dz_{i,k-u}}{O(\bar{\ell}_{k-u,n}) - O(\underline{\ell}_{k-u,n})} \\ &\triangleq \mathfrak{N}_{i,k-u|a}. \end{aligned}$$

Furthermore, one has

$$\begin{aligned} & \mathbb{E} \left\{ z_{i,k-u}^2 \mid z_{i,k-u} \in [\underline{\ell}_{k-u,n}, \bar{\ell}_{k-u,n}), x_{k-u} \right\} \\ &= \int_{\underline{\ell}_{k-u,n}}^{\bar{\ell}_{k-u,n}} z_{i,k-u}^2 \frac{o(z_{i,k-u})}{O(\bar{\ell}_{k-u,n}) - O(\underline{\ell}_{k-u,n})} dz_{i,k-u} \\ &= - \frac{\sigma_{i,k-u}^2 \int_{\underline{\ell}_{k-u,n}}^{\bar{\ell}_{k-u,n}} z_{i,k-u} \frac{-(z_{i,k-u} - \mu_{i,k-u})}{\sigma_{i,k-u}^2} o(z_{i,k-u}) dz_{i,k-u}}{O(\bar{\ell}_{k-u,n}) - O(\underline{\ell}_{k-u,n})} + \mu_{i,k-u} \int_{\underline{\ell}_{k-u,n}}^{\bar{\ell}_{k-u,n}} z_{i,k-u} \frac{o(z_{i,k-u})}{O(\bar{\ell}_{k-u,n}) - O(\underline{\ell}_{k-u,n})} dz_{i,k-u} \\ &\triangleq \mathfrak{h}_{i,k-u|a}. \end{aligned}$$

Then, it is obtained that

$$\begin{aligned} & \mathbb{E} \left\{ D_{i,k-\tau}^2 \mid z_{i,k-u} \in [\underline{\ell}_{k-u,n}, \bar{\ell}_{k-u,n}), x_{k-u} \right\} \\ &= \mathbb{E} \left\{ \left(\frac{1}{\eta_{k-u}} z_{i,k-u} - n\zeta \right)^2 \mid z_{i,k-u} \in [\underline{\ell}_{k-u,n}, \bar{\ell}_{k-u,n}), x_{k-u} \right\} \\ &\triangleq \mathfrak{S}_{i,k-u|a}. \end{aligned}$$

Similarly, when $z_{i,k-u} \geq \vartheta_{k-u}$ and $z_{i,k-u} < -\vartheta_{k-u}$, we have

$$\mathbb{E} \left\{ D_{i,k-\tau}^2 \mid z_{i,k-u} \geq \vartheta_{k-u}, x_{k-u} \right\} \triangleq \mathfrak{S}_{i,k-u|b}$$

and

$$\mathbb{E} \left\{ D_{i,k-\tau}^2 \mid z_{i,k-u} < -\vartheta_{k-u}, x_{k-u} \right\} \triangleq \mathfrak{S}_{i,k-u|c}.$$

Appendix B Proof of Theorem 2

By using Lemma 1, we have

$$\begin{aligned} & \mathbb{E} \{ \Upsilon_{1,k+1} + \Upsilon_{1,k+1}^T \} \\ & \leq \alpha_1 (I - \mathcal{L}_{k+1} \mathcal{C}_{k+1}) \mathcal{P}_{k+1|k} (I - \mathcal{L}_{k+1} \mathcal{C}_{k+1})^T + \alpha_1^{-1} \mathcal{L}_{k+1} \mathcal{C}_{k+1} \mathcal{P}_{k+1|k} \mathcal{C}_{k+1}^T \mathcal{L}_{k+1}^T, \\ & \mathbb{E} \{ -\Upsilon_{2,k+1} - \Upsilon_{2,k+1}^T \} \\ & \leq \alpha_2 (I - \mathcal{L}_{k+1} \mathcal{C}_{k+1}) \mathcal{P}_{k+1|k} (I - \mathcal{L}_{k+1} \mathcal{C}_{k+1})^T + \alpha_2^{-1} \mathcal{L}_{k+1} \mathcal{C}_{k+1-u} \mathcal{P}_{k+1-u|k-u} \mathcal{C}_{k+1-u}^T \mathcal{L}_{k+1}^T, \\ & \mathbb{E} \{ \Upsilon_{3,k+1} + \Upsilon_{3,k+1}^T \} \\ & \leq \alpha_3 (I - \mathcal{L}_{k+1} \mathcal{C}_{k+1}) \mathcal{P}_{k+1|k} (I - \mathcal{L}_{k+1} \mathcal{C}_{k+1})^T + \alpha_3^{-1} \mathcal{L}_{k+1} \eta_{k+1-u} \mathbb{E} \{ D_{k+1-\tau} D_{k+1-\tau}^T \} \eta_{k+1-u}^T \mathcal{L}_{k+1}^T, \\ & \mathbb{E} \{ -\Upsilon_{4,k+1} - \Upsilon_{4,k+1}^T \} \\ & \leq \alpha_4 \mathcal{L}_{k+1} \mathcal{C}_{k+1} \mathcal{P}_{k+1|k} \mathcal{C}_{k+1}^T \mathcal{L}_{k+1}^T + \alpha_4^{-1} \mathcal{L}_{k+1} \mathcal{C}_{k+1-u} \mathcal{P}_{k+1-u|k-u} \mathcal{C}_{k+1-u}^T \mathcal{L}_{k+1}^T, \\ & \mathbb{E} \{ \Upsilon_{5,k+1} + \Upsilon_{5,k+1}^T \} \\ & \leq \alpha_5 \mathcal{L}_{k+1} \mathcal{C}_{k+1} \mathcal{P}_{k+1|k} \mathcal{C}_{k+1}^T \mathcal{L}_{k+1}^T + \alpha_5^{-1} \mathcal{L}_{k+1} \eta_{k+1-u} \mathbb{E} \{ D_{k+1-\tau} D_{k+1-\tau}^T \} \eta_{k+1-u}^T \mathcal{L}_{k+1}^T, \\ & \mathbb{E} \{ -\Upsilon_{6,k+1} - \Upsilon_{6,k+1}^T \} \\ & \leq \alpha_6 \mathcal{L}_{k+1} \mathcal{Q}_{k+1-u} \mathcal{L}_{k+1}^T + \alpha_6^{-1} \mathcal{L}_{k+1} \eta_{k+1-u} \mathbb{E} \{ D_{k+1-\tau} D_{k+1-\tau}^T \} \eta_{k+1-u}^T \mathcal{L}_{k+1}^T, \\ & \mathbb{E} \{ -\Upsilon_{7,k+1} - \Upsilon_{7,k+1}^T \} \\ & \leq \alpha_7 \mathcal{L}_{k+1} \mathcal{C}_{k+1-u} \mathcal{P}_{k+1-u|k-u} \mathcal{C}_{k+1-u}^T \mathcal{L}_{k+1}^T + \alpha_7^{-1} \mathcal{L}_{k+1} \eta_{k+1-u} \mathbb{E} \{ D_{k+1-\tau} D_{k+1-\tau}^T \} \eta_{k+1-u}^T \mathcal{L}_{k+1}^T. \end{aligned} \tag{B1}$$

Applying (B1) and Lemma 3 to (17) yields

$$\begin{aligned} \mathcal{P}_{k+1|k+1} &\leq \delta_1(I - \mathcal{L}_{k+1}\mathcal{C}_{k+1})\mathcal{P}_{k+1|k}(I - \mathcal{L}_{k+1}\mathcal{C}_{k+1})^T + \delta_5\mathcal{L}_{k+1}\mathcal{C}_{k+1-u}\mathcal{P}_{k+1-u|k-u}\mathcal{C}_{k+1-u}^T\mathcal{L}_{k+1}^T \\ &\quad + \delta_2\mathcal{L}_{k+1}\mathcal{C}_{k+1}\mathcal{P}_{k+1|k}\mathcal{C}_{k+1}^T\mathcal{L}_{k+1}^T + \delta_4\eta_{k+1-u}^2 \sum_{i=1}^{n_z} \mathfrak{S}_{i,k+1-u}\mathcal{L}_{k+1}\mathcal{C}_{k+1}^T + \delta_3\mathcal{L}_{k+1}\mathcal{Q}_{k+1-u}\mathcal{L}_{k+1}^T. \end{aligned} \quad (\text{B2})$$

Then, based on Lemma 2, (14), (18), (19), and (B2), one has

$$\mathcal{P}_{k+1|k+1} \leq \Theta_{k+1|k+1}.$$

Finally, in light of the completing-the-square method, we have

$$\begin{aligned} \Theta_{k+1|k+1} &= \mathcal{L}_{k+1}\mathcal{M}_{k+1}\mathcal{L}_{k+1} - \delta_1\Theta_{k+1|k}\mathcal{C}_{k+1}^T\mathcal{L}_{k+1}^T - \delta_1\mathcal{L}_{k+1}\mathcal{C}_{k+1}\Theta_{k+1|k} + \delta_1\Theta_{k+1|k} \\ &= (\mathcal{L}_{k+1} - \delta_1\Theta_{k+1|k}\mathcal{C}_{k+1}^T\mathcal{M}_{k+1}^{-1})\mathcal{M}_{k+1}(\mathcal{L}_{k+1} - \delta_1\Theta_{k+1|k}\mathcal{C}_{k+1}^T\mathcal{M}_{k+1}^{-1})^T \\ &\quad - \delta_1^2\Theta_{k+1|k}\mathcal{C}_{k+1}^T\mathcal{M}_{k+1}^{-1}\mathcal{C}_{k+1}\Theta_{k+1|k} + \delta_1\Theta_{k+1|k}. \end{aligned} \quad (\text{B3})$$

For the sake of minimizing the UB $\Theta_{k+1|k+1}$, it is not difficult to calculate the filter gain \mathcal{L}_{k+1} from (B3).

Appendix C Proof of Theorem 3

The filtering error $e_{k+1|k+1}$ can be rewritten by (16) and (17) as

$$\begin{aligned} e_{k+1|k+1} &= \mathcal{H}_k e_{k|k} + \mathcal{B}_k w_k - \mathcal{L}_{k+1}\mathcal{C}_{k+1-u}\mathcal{H}_{k-u}e_{k-u|k-u} - \mathcal{L}_{k+1}\mathcal{C}_{k+1-u}\mathcal{B}_{k-u}w_{k-u} - \mathcal{L}_{k+1}v_{k+1-u} \\ &\quad + \mathcal{L}_{k+1}\eta_{k+1-u}D_{k+1-\tau}. \end{aligned} \quad (\text{C1})$$

From (20), it is derived that

$$\begin{aligned} \|\mathcal{L}_{k+1}\| &= \left\| \delta_1\Theta_{k+1|k}\mathcal{C}_{k+1}\mathcal{M}_{k+1}^{-1} \right\| \\ &< \left\| \delta_1\Theta_{k+1|k}\mathcal{C}_{k+1} \right\| \left\| [\delta_1\mathcal{C}_{k+1}\Theta_{k+1|k}\mathcal{C}_{k+1}^T]^{-1} \right\| \end{aligned} \quad (\text{C2})$$

$$\leq \frac{\bar{\theta}\bar{c}}{\underline{\theta}\underline{c}^2} \triangleq \iota. \quad (\text{C3})$$

We define a recursive function about Ψ_k :

$$\Psi_{k+1} \triangleq \mathcal{H}_k\Psi_k\mathcal{H}_k^T + \mathcal{B}_kR_k\mathcal{B}_k^T + \gamma I, \quad (\text{C4})$$

where $\Psi_0 \triangleq \mathcal{B}_0Q_0\mathcal{B}_0^T + \gamma I$ and $\gamma > 0$.

By the properties of the matrix norm, we have

$$\|\Psi_{k+1}\| \leq \|\mathcal{H}_{k+1}\|^2\|\Psi_k\| + \|\mathcal{B}_kR_k\mathcal{B}_k^T\| + \|\gamma I\| \leq \bar{h}^2\|\Psi_k\| + \bar{b}^2\bar{\tau} + \gamma. \quad (\text{C5})$$

In addition, it follows from (C4) that

$$\Psi_k \geq \gamma I. \quad (\text{C6})$$

By means of (21) and Lemma 4, $\psi I \leq \Psi_k \leq \bar{\psi} I$, where ψ and $\bar{\psi}$ are two positive scalars.

Subsequently, a quadratic function is constructed as follows:

$$V_k(e_{k|k}) \triangleq e_{k|k}^T \Psi_k^{-1} e_{k|k}. \quad (\text{C7})$$

Applying (C1) to (C7), one has

$$\begin{aligned} &\mathbb{E}\{V_{k+1}(e_{k+1|k+1})|e_{k|k}\} - (1 + \beta)V_k(e_{k|k}) \\ &= \mathbb{E}\{e_{k|k}^T \mathcal{H}_k^T \Psi_{k+1}^{-1} \mathcal{H}_k e_{k|k} + w_k^T \mathcal{B}_k^T \Psi_{k+1}^{-1} \mathcal{B}_k w_k + e_{k-u|k-u}^T \mathcal{H}_{k-u}^T \mathcal{C}_{k+1-u}^T \mathcal{L}_{k+1}^T \Psi_{k+1}^{-1} \mathcal{L}_{k+1} \mathcal{C}_{k+1-u} \mathcal{H}_{k-u} e_{k-u|k-u} \\ &\quad + v_{k+1-u}^T \mathcal{L}_{k+1}^T \Psi_{k+1}^{-1} \mathcal{L}_{k+1} v_{k+1-u} + w_{k-u}^T \mathcal{B}_{k-u}^T \mathcal{C}_{k+1-u}^T \mathcal{L}_{k+1}^T \Psi_{k+1}^{-1} \mathcal{L}_{k+1} \mathcal{C}_{k+1-u} \mathcal{B}_{k-u} w_{k-u} \\ &\quad + D_{k+1-\tau}^T \eta_{k+1-u}^T \mathcal{L}_{k+1}^T \Psi_{k+1}^{-1} \mathcal{L}_{k+1} \eta_{k+1-u} D_{k+1-\tau} - \Xi_{1,k+1} - \Xi_{1,k+1}^T - \Xi_{2,k+1} - \Xi_{2,k+1}^T \\ &\quad - \Xi_{3,k+1} - \Xi_{3,k+1}^T - \Xi_{4,k+1} - \Xi_{4,k+1}^T - (1 + \beta)e_{k|k}^T \Psi_k^{-1} e_{k|k}\}, \end{aligned} \quad (\text{C8})$$

where

$$\begin{aligned} \Xi_{1,k+1} &= e_{k|k}^T \mathcal{H}_k^T \Psi_{k+1}^{-1} \mathcal{L}_{k+1} \mathcal{C}_{k+1-u} \mathcal{H}_{k-u} e_{k-u|k-u}, \\ \Xi_{2,k+1} &= e_{k|k}^T \mathcal{H}_k^T \Psi_{k+1}^{-1} \mathcal{L}_{k+1} \mathcal{C}_{k+1-u} \mathcal{B}_{k-u} w_{k-u}, \\ \Xi_{3,k+1} &= w_{k-u}^T \mathcal{B}_{k-u}^T \mathcal{C}_{k+1-u}^T \Psi_{k+1}^{-1} \mathcal{L}_{k+1} \eta_{k+1-u} D_{k+1-\tau}, \\ \Xi_{4,k+1} &= v_{k+1-u}^T \mathcal{L}_{k+1}^T \Psi_{k+1}^{-1} \mathcal{L}_{k+1} \eta_{k+1-u} D_{k+1-\tau}. \end{aligned}$$

Similarly, according to Lemma 1, one has

$$\begin{aligned}
 & \mathbb{E} \left\{ -\Xi_{1,k+1} - \Xi_{1,k+1}^T \right\} \\
 & \leq \sigma_1 e_{k|k}^T \mathcal{H}_k^T \Psi_{k+1}^{-1} \mathcal{H}_k e_{k|k} + \sigma_1^{-1} e_{k-u|k-u}^T \mathcal{H}_{k-u}^T \mathcal{C}_{k+1-u}^T \mathcal{L}_{k+1}^T \Psi_{k+1}^{-1} \mathcal{L}_{k+1} \mathcal{C}_{k+1-u} \mathcal{H}_{k-u} e_{k-u|k-u}, \\
 & \mathbb{E} \left\{ -\Xi_{2,k+1} - \Xi_{2,k+1}^T \right\} \\
 & \leq \sigma_2 e_{k|k}^T \mathcal{H}_k^T \Psi_{k+1}^{-1} \mathcal{H}_k^T e_{k|k} + \sigma_2^{-1} w_{k-u}^T \mathcal{B}_{k-u}^T \mathcal{C}_{k+1-u}^T \mathcal{L}_{k+1}^T \Psi_{k+1}^{-1} \mathcal{L}_{k+1} \mathcal{C}_{k+1-u} \mathcal{B}_{k-u} w_{k-u}, \\
 & \mathbb{E} \left\{ -\Xi_{3,k+1} - \Xi_{3,k+1}^T \right\} \\
 & \leq \sigma_3 w_{k-u}^T \mathcal{B}_{k-u}^T \mathcal{L}_{k+1}^T \Psi_{k+1}^{-1} \mathcal{L}_{k+1} \mathcal{B}_{k-u} w_{k-u} + \sigma_3^{-1} \eta_{k+1-u}^2 D_{k+1-\tau}^T \mathcal{L}_{k+1}^T \Psi_{k+1}^{-1} \mathcal{L}_{k+1} D_{k+1-\tau}, \\
 & \mathbb{E} \left\{ -\Xi_{4,k+1} - \Xi_{4,k+1}^T \right\} \\
 & \leq \sigma_4 v_{k+1-u}^T \mathcal{L}_{k+1}^T \Psi_{k+1}^{-1} \mathcal{L}_{k+1} v_{k+1-u} + \sigma_4^{-1} \eta_{k+1-u}^2 D_{k+1-\tau}^T \mathcal{L}_{k+1}^T \Psi_{k+1}^{-1} \mathcal{L}_{k+1} D_{k+1-\tau},
 \end{aligned} \tag{C9}$$

where $\sigma_1 = \sigma_2 = \beta/2$, σ_3 and σ_4 are positive scalars.

The following inequalities can be obtained from the property of the matrix trace:

$$\begin{aligned}
 & \mathbb{E} \left\{ w_k^T \mathcal{B}_k^T \Psi_{k+1}^{-1} \mathcal{B}_k w_k \right\} \leq n_x \bar{r} \bar{b}^2 \underline{\psi}, \\
 & \mathbb{E} \left\{ v_{k+1-u}^T \mathcal{L}_{k+1}^T \Psi_{k+1}^{-1} \mathcal{L}_{k+1} v_{k+1-u} \right\} \leq n_z \bar{q} \bar{l}^2 \underline{\psi}, \\
 & \mathbb{E} \left\{ e_{k-u|k-u}^T \mathcal{H}_{k-u}^T \mathcal{C}_{k+1-u}^T \mathcal{L}_{k+1}^T \Psi_{k+1}^{-1} \mathcal{L}_{k+1} \mathcal{C}_{k+1-u} \mathcal{H}_{k-u} e_{k-u|k-u} \right\} \leq n_x \bar{\omega} \bar{h}^2 \bar{l}^2 \bar{c}^2 \underline{\psi}, \\
 & \mathbb{E} \left\{ \eta_{k+1-u}^2 D_{k+1-\tau}^T \mathcal{L}_{k+1}^T \Psi_{k+1}^{-1} \mathcal{L}_{k+1} D_{k+1-\tau} \right\} \leq n_z \eta^2 \bar{l}^2 \underline{\psi} \zeta^2 / 4, \\
 & \mathbb{E} \left\{ w_{k-u}^T \mathcal{B}_{k-u}^T \mathcal{C}_{k+1-u}^T \mathcal{L}_{k+1}^T \Psi_{k+1}^{-1} \mathcal{L}_{k+1} \mathcal{C}_{k+1-u} \mathcal{B}_{k-u} w_{k-u} \right\} \leq n_x \bar{r} \bar{b}^2 \bar{c}^2 \bar{l}^2 \underline{\psi}.
 \end{aligned} \tag{C10}$$

Based on the matrix inversion lemma, one obtains

$$\begin{aligned}
 & \mathcal{H}_k^T \Psi_{k+1}^{-1} \mathcal{H}_k - \Psi_k^{-1} \\
 & = \mathcal{H}_k^T (\mathcal{H}_k \Psi_k \mathcal{H}_k^T + \mathcal{B}_k R_k \mathcal{B}_k^T + \gamma I)^{-1} \mathcal{H}_k - \Psi_k^{-1} \\
 & = -[\Psi_k + \Psi_k \mathcal{H}_k^T (\mathcal{B}_k R_k \mathcal{B}_k^T + \gamma I)^{-1} \mathcal{H}_k \Psi_k]^{-1} \\
 & = -[I + \mathcal{H}_k^T (\mathcal{B}_k R_k \mathcal{B}_k^T + \gamma I)^{-1} \mathcal{H}_k \Psi_k]^{-1} \Psi_k^{-1} \\
 & \leq - \left(1 + \frac{\bar{h}^2 \bar{\psi}}{\bar{l}^2 \bar{r}} \right)^{-1} \Psi_k^{-1}.
 \end{aligned} \tag{C11}$$

Taking Lemma 4 and (C9)–(C11) into consideration, one has

$$\begin{aligned}
 & \mathbb{E} \{ V_{k+1}(e_{k+1|k+1}) | e_{k|k} \} - (1 + \beta) V_k(e_{k|k}) \\
 & \leq \mathbb{E} \{ (1 + \beta) e_{k|k}^T [\mathcal{H}_k^T \Psi_{k+1}^{-1} \mathcal{H}_k - \Psi_k^{-1}] e_{k|k} + (1 + 2\beta^{-1}) e_{k-u|k-u}^T \mathcal{H}_{k-u}^T \mathcal{C}_{k+1-u}^T \mathcal{L}_{k+1}^T \Psi_{k+1}^{-1} \mathcal{L}_{k+1} \mathcal{C}_{k+1-u} \mathcal{H}_{k-u} e_{k-u|k-u} \\
 & \quad + \sigma_4 v_{k+1-u}^T \mathcal{L}_{k+1}^T \Psi_{k+1}^{-1} \mathcal{L}_{k+1} v_{k+1-u} + (1 + 2\beta^{-1} + \sigma_3) w_{k-u}^T \mathcal{B}_{k-u}^T \mathcal{C}_{k+1-u}^T \mathcal{L}_{k+1}^T \Psi_{k+1}^{-1} \mathcal{L}_{k+1} \mathcal{C}_{k+1-u} \mathcal{B}_{k-u} w_{k-u} \\
 & \quad + w_k^T \mathcal{B}_k \Psi_{k+1}^{-1} \mathcal{B}_k w_k + (\sigma_3^{-1} + \sigma_4^{-1}) \eta_{k+1-u}^2 D_{k+1-\tau}^T \mathcal{L}_{k+1}^T \Psi_{k+1}^{-1} \mathcal{L}_{k+1} D_{k+1-\tau} \} \\
 & \leq -(1 + \beta) \left(1 + \frac{\bar{h}^2 \bar{\psi}}{\bar{l}^2 \bar{r}} \right)^{-1} V_k(e_{k|k}) + \varrho,
 \end{aligned} \tag{C12}$$

which means that

$$\mathbb{E} \{ V_{k+1}(e_{k+1|k+1}) | e_{k|k} \} \leq \nu V_k(e_{k|k}) + \varrho,$$

where

$$\begin{aligned}
 \nu & = (1 + \beta) \left[1 - \left(1 + \frac{\bar{h}^2 \bar{\psi}}{\bar{l}^2 \bar{r}} \right)^{-1} \right], \\
 \varrho & = (1 + 2\beta^{-1}) n_x \bar{\omega} \bar{h}^2 \bar{c}^2 \bar{l}^2 \underline{\psi} + (1 + 2\beta^{-1} + \sigma_3) n_x \bar{r} \bar{b}^2 \bar{c}^2 \bar{l}^2 \underline{\psi} \\
 & \quad + n_x \bar{r} \bar{b}^2 \underline{\psi} + \sigma_4 n_z \bar{q} \bar{l}^2 \underline{\psi} + (\sigma_3^{-1} + \sigma_4^{-1}) n_z \eta^2 \bar{l}^2 \underline{\psi} \zeta^2 / 4.
 \end{aligned}$$

It is obvious that $0 < \nu < 1$ for some $\beta > 0$. Consequently, in light of Lemma 4, the filtering error is MSEB.